Pressure-enhanced electronic coupling of highly passivated quantum dot films to improve photovoltaic performance

Yinglin Wang (iD), Meiqi An, Yuwen Jia (iD), Lei Wang, Jinhuan Li, Binbin Weng (iD), Xintong Zhang (iD), and Yichun Liu

View Online   Export Citation   CrossMark

ARTICLES YOU MAY BE INTERESTED IN

Effect of glycerol on the mechanical and temperature-sensing properties of pectin films
Applied Physics Letters 115, 193702 (2019); https://doi.org/10.1063/1.5121710

Ohmic contact to AlN:Si using graded AlGaN contact layer
Applied Physics Letters 115, 192104 (2019); https://doi.org/10.1063/1.5124936

High on/off ratio black phosphorus based memristor with ultra-thin phosphorus oxide layer
Applied Physics Letters 115, 193503 (2019); https://doi.org/10.1063/1.5115531

AIP Publishing

Pressure-enhanced electronic coupling of highly passivated quantum dot films to improve photovoltaic performance

View Online   Export Citation   CrossMark

Yinglin Wang,[1,a)] (iD) Meiqi An,[1,a)] Yuwen Jia,[1] (iD) Lei Wang,[1] Jinhuan Li,[1] Binbin Weng,[2] (iD) Xintong Zhang,[1,b)] (iD) and Yichun Liu[1,b)]

AFFILIATIONS

[1]Center for Advanced Optoelectronic Materials Research, School of Physics, and Key Laboratory of UV-Emitting Materials and Technology of Ministry of Education, Northeast Normal University, 5268 Renmin Street, Changchun 130024, China
[2]School of Electrical and Computer Engineering, University of Oklahoma, 660 Parrington Oval, Norman, Oklahoma 73019-0390, USA

a)**Contributions:** Y. Wang and M. An contributed equally to this work.
b)**Authors to whom correspondence should addressed:** xtzhang@nenu.edu.cn and ycliu@nenu.edu.cn

ABSTRACT

PbS colloidal quantum dot solar cells (CQDSCs) have recently achieved remarkable performance enhancement due to the development of the phase-transfer ligand exchange (PTLE) method. However, the lack of compact packing of the PTLE-passivated CQDs impairs the interdot electronic coupling and thereby severely restricts further improvement in performance. To address this electronic coupling issue, we report a simple yet effective process of external pressure (0–2 MPa). We find that the interdot distance is reduced after the application of the pressure. Both optical and electrical measurements clearly demonstrate that the distance reduction can effectively strengthen the interdot electronic coupling, thus promoting the carrier transport of the CQD layer. However, too much pressure (>2 MPa) could accelerate the detrimental carrier recombination processes of CQDSCs. Accordingly, by optimizing the carrier transport and recombination processes, we achieve the maximum power conversion efficiency of 8.2% with a moderate pressure of 1.5 MPa, which is 25.5% higher than the solar cell without the external pressure. This effective strategy of external pressure could also be applied to other CQD-based optoelectronic devices to realize a better device performance.

Published under license by AIP Publishing. https://doi.org/10.1063/1.5110749

Colloidal quantum dots (CQDs) are of interest for applications in low-cost, solution-processable photonic, and electronic devices[1–3] due to their size-tunable bandgap,[4] high extinction coefficient,[5] and multiple exciton generation.[6] In particular, lead sulfide (PbS) CQDs have attracted great attention in the photovoltaic field because of their remarkable ambient stability[7,8] and optical absorption in the near- to mid-infrared range.[9,10] The main bottleneck of PbS colloidal quantum dot solar cells (CQDSCs) is the insufficient electronic coupling between neighboring CQDs.[11–13] Consequently, the chemical replacement of the insulating long-chain ligands of the as-synthesized CQDs by smaller molecules and/or ions is essential for the fabrication of CQDSCs.[14,15] At one time, this type of ligand exchange was performed in films that required multiple processes of layer-by-layer deposition to obtain a sufficiently thick CQD film. As a result, this method usually caused issues with film cracking and high material consumption. In addition, this solid-state ligand exchange (SSLE) method may generate surface traps of PbS CQDs because of the imperfect passivation and cause power loss of CQDSCs.[16–18]

Recently, an advanced phase-transfer ligand exchange (PTLE) method has been developed to realize the single-step deposition of CQD films with an unprecedented thickness and smoothness.[19–22] The PTLE method can suppress the trap-related carrier recombination, improve the carrier transport in the PbS CQDSCs, and thereby dramatically improve the photovoltaic performance.[23,24] To date, great attention has been paid to the chemical optimization of the PTLE process for efficient trap passivation, but the issues of CQD stacking in the obtained films are still unresolved. It is notable that the single-step deposition and rapid solvent evaporation during the fabrication of a CQD film may result in the loose stacking of CQDs and thus lead to an insufficient interdot electron coupling. When considering the mismatch between the limited carrier transport length ($\sim$350 nm)[13] in well-passivated CQD films and the desired light-harvesting thickness of the PbS CQD film ($\sim$1 μm),[25] further enhancement of electron coupling is very crucial to obtain high-performance PbS CQDSCs.
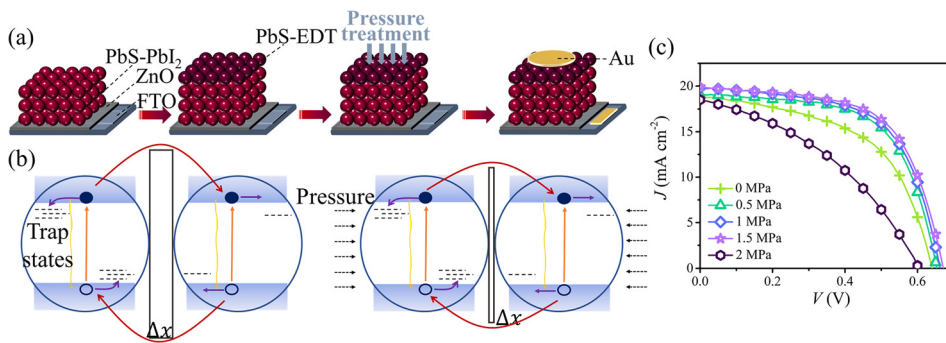
FIG. 1. (a) Schematic of CQDSC fabrication. (b) Variation of interdot electronic coupling, and recombination induced by the pressure. (c) Best-performing current density-voltage scans of PbS CQDSCs treated with different pressures.

To enhance the interdot electron coupling, we developed a strategy of applying external pressure on the PbS CQDSCs to realize the dense packing of CQD films prepared by the PTLE method. The power conversion efficiency (PCE) was increased to 8.2% when the external pressure reached 1.5 MPa in contrast to that of 6.5% without applying the pressure. The external pressure could reduce the interdot distance and enhance the electronic coupling in sequence when the pressure increases from 0 to 2 MPa. However, continuing to increase the pressure will cause a critical problem of carrier recombination probably due to the facilitated carrier transport to the traps of CQDs and/or the pressure-induced microstructural defects of CQDSCs. This after-the-fact treatment with a moderate pressure could be conveniently performed with normal equipment. It could be integrated with other automated fabrication processes of CQD films, such as ink jet printing and slot die coating, to realize line production of high-performance CQD-based optoelectronic devices.

Figure 1(a) shows a schematic of the architecture of PbS CQDSCs and the process of external pressure after the fact. The PbS CQDs (Fig. S1, supplementary material) were prepassivated by PbI_2 through the PTLE method (called PbS-PbI_2) and spin coated on the ZnO electron extraction layer. Another hole extraction layer of PbS CQDs capped with 1, 2-ethanedithiol ligands (called PbS-EDT) was deposited on top of the PbS-PbI_2 absorber layer by the SSLE method. Then, the obtained FTO/ZnO/PbS-PbI_2/PbS-EDT multilayer films were treated with mechanical pressure that increased from 0 to 2 MPa using the tablet machine. Finally, Au electrodes (~100 nm) were evaporated on the surface of the PbS-EDT layer.

We first evaluated the influence of the increasing pressure on the CQDSCs by using the current density–voltage (J–V) curves [Fig. 1(c), Fig. S2, and Table SI]. As the pressure increased from 0 to 1.5 MPa, the short-circuit current density (J_{sc}) monotonically rose from 18.87 to 19.91 mA/cm^2, while the open-circuit voltage (V_{oc}) increased from 0.64 to 0.67 V. This variation of J_{sc} is further confirmed by the external quantum efficiency measurements (Fig. S3). The fill factor (FF) increased to ~0.61 after application of the pressure in contrast to that of 0.54 for the untreated solar cell. Consequently, the maximum PCE of 8.17% was obtained as the pressure reached 1.5 MPa, generating an increase in 25.5% over the PCE of CQDSCs without the application of pressure (6.51%). However, the further increase in pressure to 2 MPa caused obvious drops of J_{sc}, V_{oc}, and FF, and thus dramatically reduced PCE to 4.74%.

To understand this variation of photovoltaic performance, we characterized both the pressure-dependent optical [Fig. 2(a)] and electrical properties [Fig. 2(b)] of PbS-PbI_2 CQD films. The position and full width at half maximum of the first exciton absorption peaks of PbS-PbI_2 films remained unchanged after application of the external pressure, showing that the external pressure induced negligible change in the size distribution of PbS-PbI_2 CQDs. However, the photoluminescence (PL) peaks of PbS-PbI_2 films did shift continuously from 1131 to 1167 nm as the external pressure increased (Fig. S4). The rapid solvent evaporation during the preparation process of PbS CQD films usually leads to a lack of compact packing of PbS CQDs, but our process of external pressure made the PbS CQD films denser and thus reduced the interdot distance. The thickness of PbS-PbI_2 CQD films shrinks after the external pressure process, clearly confirming this pressure-induced reduction of the interdot distance (Fig. S5). In addition, we found that the process of external pressure increased the refractive index of PbS CQD films (Figs. S6 and S7). By considering
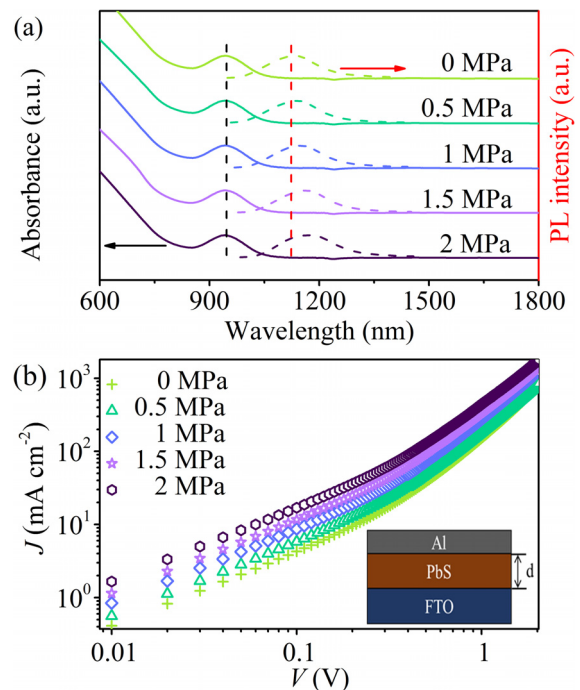

FIG. 2. (a) Pressure-dependent absorption and PL spectra of PbS CQD films. (b) Pressure-dependent J–V curves of PbS CQD films. Inset: device structure used in this experiment.

the unchanged size distribution and surface ligand of PbS CQDs under different conditions of external pressure, the only possible explanation for the refractive index increase along with the pressure rise is the reduction of the interdot distance in the CQD layer.

The rate of carrier transport based on the hopping mechanism in the CQD films is proportional to the interdot distance.[26] As a result, shortening the interdot distance by applying the external pressure can enhance the interdot coupling and promote the carrier transfer in the PbS CQD films. Since the change in the size distribution of PbS CQDs is negligible, the redshift in PL peaks may result from the enhancement of interdot electronic coupling which facilitates the transport of photo-generated carriers to the PbS CQDs with small band gaps. Such a red-shift of PL peaks in well-coupled CQD films has also been reported in the previous literature.[27,28] It is worthwhile to note that the PL intensity of PbS-PbI$_2$ CQD films reduces continuously with the increase in pressure, as shown in Fig. S8(a). This reduction of PL intensity might derive from the additional channels (carrier transfer to the neighboring CQDs) of nonradiative decay in the well-coupled CQD films as shown in Fig. 1(b). In addition, the higher refractive index of the denser PbS CQD films may increase the reflection loss of exciting light and the confine-ment of PL inside the films. Using the space charge limited current (SCLC) measurement,[29] we estimated the carrier mobility (μ_n) of PbS CQD films which increased from 2.37×10^{-3} cm^2/V s to 6.75×10^{-3} cm^2/V s as the pressure increased from 0 to 2 MPa (Table SII). Correspondingly, both photonic and electrical measurements showed that the application of pressure could reduce the interdot distance and enhance electronic coupling between neighboring PbS CQDs.

To investigate the influence of pressure-dependent electronic coupling on the functioning mechanism of CQDSCs, we used several techniques to characterize the devices. The density of states (DOS) for CQDSCs were extracted from the slope of capacitance-voltage plots [Fig. 3(a)], which increased from 1.68×10^{16} (0 MPa) to 2.58 $\times 10^{16}$ cm^{-3} (2 MPa) [Fig. 3(b)]. In addition, the simplified devices with a structure of SnO$_2$:F conductive substrate (FTO)/ZnO/PbS-PbI$_2$/ Au also present a DOS reduction of PbS-PbI$_2$ CQD films with an increase in pressure (Fig. S9). Because of the similar passivation pro-cesses of PbS CQDs used in this work, the increase in DOS unlikely results from the variation in the surface traps of PbS CQDs. The increase in DOS, after the pressure is applied, might derive from the incremental numbers of PbS CQDs per unit volume due to the shrink-ing of CQDs films (Fig. S5). By fitting the dark J–V curves (Fig. S10) with the ideal diode equation,[30,31] we obtained that the series resistances (R_s) reduced from 7.3 to 4.1 Ω cm^2 when the pressure increased [Fig. 3(c)]. This variation of R_s correlates well with the enhancement of car-rier transport in the PbS CQD films and may lead to an increase in J_{sc} and FF as the pressure increases from 0 to 1.5 MPa. However, we notice that the abnormal variation of shunt resistance (R_{sh}) and reverse satu-ration current density (J_0) were obtained at a pressure of 2.0 MPa [Figs. 3(c) and 3(d)]. These values suggest that although the application of the pressure improves the carrier transport, it could accelerate the unwanted carrier recombination of CQDSCs.

We then measured the transient photovoltage (TPV) to further study the carrier recombination of CQDSCs. The recombination life-times (τ_{rec}) under different light intensities were fit to a single expo-nential decay of V_{oc}. As illustrated in Fig. 4(a), the maximum τ_{rec} appears when the pressure is 1.5 MPa. This change in τ_{rec} indicates that application of an appropriate pressure could efficiently attenuate
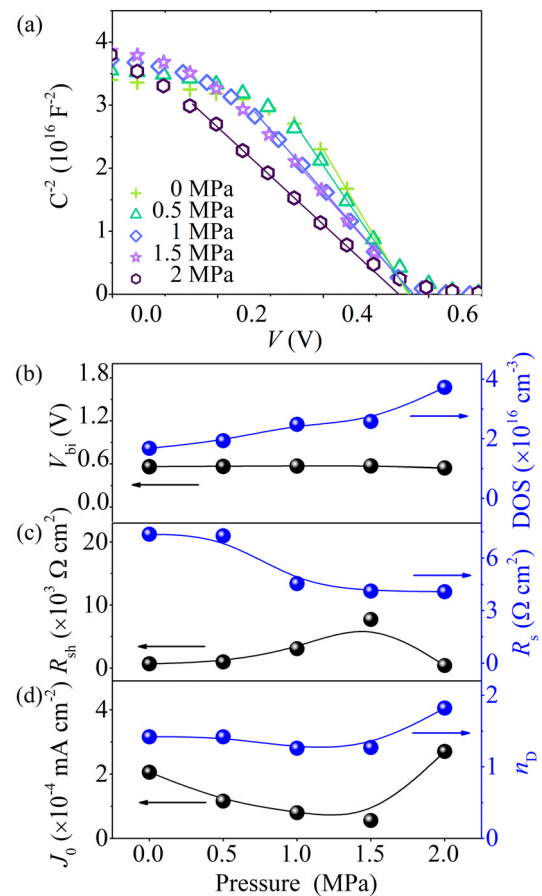

FIG. 3. (a) Pressure-dependent Mott–Schottky plots of PbS CQDSCs, and the cor-responding (b) V_{bi}, DOS. (c) R_{sh}, R_s, (d) J_0, and n_D were obtained by the ideal diode equation from dark J–V curves.

the carrier recombination of CQDSCs. The dependence of J_{sc} on the light intensity can be expressed as $J_{sc} \propto I^\alpha$, where I and α are the light intensity and the exponential factor, respectively. The improved α for CQDSCs for pressures up to 1.5 MPa clearly indicates that the carrier recombination under the short-circuit condition is efficiently sup-pressed using this new process of applying pressure [Fig. 4(b)]. However, the further increase in pressure to 2 MPa leads to drops in τ_{rec} and α, which indicates the dramatic aggravation of the carrier recombination in the solar cells. This is consistent with the change of R_{sh} and J_0 and should be the origin of the observed irregular variation for the photovoltaic performance of CQDSCs.

We used the diode ideality factor as an indicator to investigate the dominant recombination mechanism of CQDSCs with the appli-cation of different pressures. As shown in Fig. 3(d), the diode ideality factors fitted from the dark J–V curves (n_D) decrease from 1.42 to 1.27 when the pressure increases from 0 to 1.5 MPa, but then rise abnor-mally to 1.82 as the pressure reaches 2 MPa. The diode ideality factors under light irradiation (n_L) present a similar variation tendency as n_D [Fig. 4(d)]. Usually the dominating recombination process of solar cells is band-to-band recombination when the diode ideality factor is
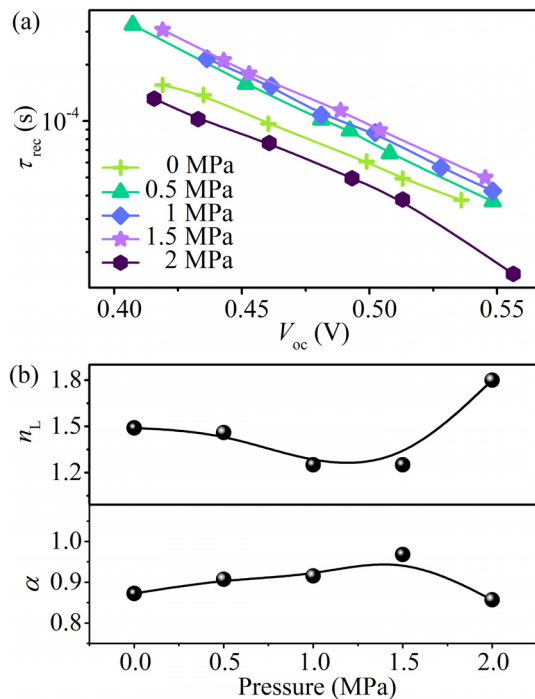
FIG. 4. (a) τ_{rec} obtained by the transient photovoltage measurements. The fitted (b) n_L and α from light-intensity depend on V_{oc} and J_{sc}.

1, whereas the recombination of solar cells is controlled by the trap-assisted process when the diode ideality factor is 2. Accordingly, the reduction of diode ideality factors along with the increase in pressure from 0 to 1.5 MPa could be ascribed to the suppressed trap-assisted recombination. However, this trap-assisted recombination becomes critical again when the pressure approaches 2 MPa.

The pressure-induced enhancement of interdot electronic coupling continuously increases the carrier mobility of PbS CQD films. However, the swift carrier transport among CQDs could increase the possibility of carrier capture by traps. Such phenomena were also observed in the certain quantum dot and organic photovoltaics.[32–34] In addition, we observed that the pressure of 2 MPa induced a reduced uniformity of PbS CQD films (Fig. S11). This may cause the microstructural defects of CQDSCs and induce extra pathways of carrier recombination. Consequently, although the PbS CQD film treated with a pressure of 2 MPa exhibits the highest μ_n, the corresponding solar cells present a dramatic drop in efficiency because of the uncontrollable carrier recombination. Accordingly, the maximum J_{sc}, V_{oc}, and thus PCE are achieved by the CQDSCs treated with a pressure of 1.5 MPa due to the acceptable balance of carrier transport and recombination.

In summary, we employed the after-the-fact external pressure treatment to efficiently solve the weak electronic coupling issue among the loose-packing PbS CQDs formed by the PTLE method. Application of external pressure shrinks the distance between the neighboring PbS CQDs and thus enhances the interdot electronic coupling. However, applying pressure that is too high induced the aggravation of the carrier recombination of CQDSCs, which may be derived from the increased

carrier capture by traps due to the inordinate enhancement of interdot electronic coupling and/or the pressure-induced microstructural defects of solar cells. As a result, a balance between carrier transport and recombination of CQDSCs could be achieved with the application of a moderate pressure of 1.5 MPa on the solar cells. This generated the maximum power conversion of 8.2% and led to an increase in 25.5% compared with that of untreated solar cells.

See the supplementary material for experimental details, UV-vis-near-infrared absorption spectrum, CQDSC photovoltaic parameter statistics, transmittance spectra, SEM images, dark J–V curves, and light intensity-dependent V_{oc} and J_{sc}.

REFERENCES

[1] S. A. McDonald, G. Konstantatos, S. Zhang, P. W. Cyr, E. J. Klem, L. Levina, and E. H. Sargent, Nat. Mater. **4**(2), 138 (2005).

[2] J. Jang, H. C. Shim, Y. Ju, J. H. Song, H. An, J. S. Yu, S. W. Kwak, T. M. Lee, I. Kim, and S. Jeong, Nanoscale **7**(19), 8829 (2015).

[3] M. Yuan, M. Liu, and E. H. Sargent, Nat. Energy **1**(3), 16016 (2016).

[4] E. M. Miller, D. M. Kroupa, J. Zhang, P. Schulz, A. R. Marshall, A. Kahn, S. Lany, J. M. Luther, M. C. Beard, C. L. Perkins, and J. van de Lagemaat, ACS Nano **10**(3), 3302 (2016).

[5] W.-K. W. C. A. Leatherdale, F. V. Mikulec, and M. G. Bawendi, J. Phys. Chem. B **106**(31), 7619 (2002).

[6] A. J. Nozik, M. C. Beard, J. M. Luther, M. Law, R. J. Ellingson, and J. C. Johnson, Chem. Rev. **110**(11), 6873 (2010).

[7] A. R. Kirmani, A. D. Sheikh, M. R. Niazi, M. A. Haque, M. Liu, F. P. G. de Arquer, J. Xu, B. Sun, O. Voznyy, N. Gasparini, D. Baran, T. Wu, E. H. Sargent, and A. Amassian, Adv. Mater. **30**(35), e1801661 (2018).

[8] C. H. Chuang, P. R. Brown, V. Bulovic, and M. G. Bawendi, Nat. Mater. **13**(8), 796 (2014).

[9] G. I. Koleilat, L. Levina, H. Shukla, S. H. Myrskog, S. Hinds, A. G. Pattantyus-Abraham, and E. H. Sargent, ACS Nano **2**(5), 833 (2008).

[10] X. Lan, S. Masala, and E. H. Sargent, Nat. Mater. **13**(3), 233 (2014).

[11] D. Zhitomirsky, O. Voznyy, S. Hoogland, and E. H. Sargent, ACS Nano **7**(6), 5282 (2013).

[12] J. J. Choi, J. Luria, B.-R. Hyun, A. C. Bartnik, L. Sun, Y.-F. Lim, J. A. Marohn, F. W. Wise, and T. Hanrath, Nano Lett. **10**(5), 1805 (2010).

[13] J. Xu, O. Voznyy, M. Liu, A. R. Kirmani, G. Walters, R. Munir, M. Abdelsamie, A. H. Proppe, A. Sarkar, F. P. Garcia de Arquer, M. Wei, B. Sun, M. Liu, O. Ouellette, R. Quintero-Bermudez, J. Li, J. Fan, L. Quan, P. Todorovic, H. Tan, S. Hoogland, S. O. Kelley, M. Stefik, A. Amassian, and E. H. Sargent, Nat. Nanotechnol. **13**(6), 456 (2018).

[14] Y. Gao, M. Aerts, C. S. S. Sandeep, E. Talgorn, T. J. Savenije, S. Kinge, L. D. A. Siebbeles, and A. J. Houtepen, ACS Nano **6**, 9606 (2012).

[15] S. Zhang, P. W. Cyr, S. A. McDonald, G. Konstantatos, and E. H. Sargent, Appl. Phys. Lett. **87**(23), 233101 (2005).

[16] D. M. Balazs and M. A. Loi, Adv. Mater. **30**(33), 1800082 (2018).

[17] H. Aqoma and S.-Y. Jang, Energy Environ. Sci. **11**(6), 1603 (2018).

[18] H. Choi, J. G. Lee, X. D. Mai, M. C. Beard, S. S. Yoon, and S. Jeong, Sci. Rep. **7**(1), 622 (2017).

[19] H. Aqoma, M. Al Mubarok, W. T. Hadmojo, E. H. Lee, T. W. Kim, T. K. Ahn, S. H. Oh, and S. Y. Jang, Adv. Mater. **29**(19), 1605756 (2017).

[20]Z. Yang, A. Janmohamed, X. Lan, F. P. Garcia de Arquer, O. Voznyy, E. Yassitepe, G. H. Kim, Z. Ning, X. Gong, R. Comin, and E. H. Sargent, Nano Lett. **15**(11), 7539 (2015).

[21]J. Tang, K. W. Kemp, S. Hoogland, K. S. Jeong, H. Liu, L. Levina, M. Furukawa, X. Wang, R. Debnath, D. Cha, K. W. Chou, A. Fischer, A. Amassian, J. B. Asbury, and E. H. Sargent, Nat. Mater. **10**(10), 765 (2011).

[22]X. Zhang, D. Jia, C. Hägglund, V. A. Öberg, J. Du, J. Liu, and E. M. J. Johansson, Nano Energy **53**, 373 (2018).

[23]W. J. Baumgardner, K. Whitham, and T. Hanrath, Nano Lett. **13**(7), 3225 (2013).

[24]Q. Lin, H. J. Yun, W. Liu, H. J. Song, N. S. Makarov, O. Isaienko, T. Nakotte, G. Chen, H. Luo, V. I. Klimov, and J. M. Pietryga, J. Am. Chem. Soc. **139**(19), 6644 (2017).

[25]I. J. Kramer and E. H. Sargent, ACS Nano **5**, 8506 (2011).

[26]J. Tang and E. H. Sargent, Adv. Mater. **23**(1), 12 (2011).

[27]H. Beygi, S. A. Sajjadi, A. Babakhani, J. F. Young, and F. C. J. M. van Veggel, Appl. Surf. Sci. **459**, 562 (2018).

[28]P. J. Roland, K. P. Bhandari, and R. J. Ellingson, J. Appl. Phys. **119**(9), 094307 (2016).

[29]M. J. Speirs, D. N. Dirin, M. Abdu-Aguye, D. M. Balazs, M. V. Kovalenko, and M. A. Loi, Energy Environ. Sci. **9**(9), 2916 (2016).

[30]J. R. Sites and P. H. Mauk, Sol. Cells **27**, 411 (1989).

[31]S. S. Hegedus and W. N. Shafarman, Prog. Photovoltaics **12**, 155 (2004).

[32]D. Zhitomirsky, O. Voznyy, L. Levina, S. Hoogland, K. W. Kemp, A. H. Ip, S. M. Thon, and E. H. Sargent, Nat. Commun. **5**, 3803 (2014).

[33]C. R. Kagan, E. Lifshitz, E. H. Sargent, and D. V. Talapin, Science **353**(6302), 885 (2016).

[34]P. N. Goswami, D. Mandal, and A. K. Rath, Nanoscale **10**(3), 1072 (2018).